ISIJ International, Vol. 43 (2003), No. 3, pp. 394–399

Effect of Undercooling of Austenite on Strain Induced Ferrite Transformation Behavior

Seung Chan HONG, Sung Hwan LIM, Kyung Jong LEE, Dong Hyuk SHIN[1)] and Kyung Sub LEE

Division of Materials Science & Engineering, Hanyang University, Seoul, Korea. E-mail: hongsc@ihanyang.ac.kr
1) Department of Metallurgy and Materials Science, Hanyang University, Ansan, Kyunggi-Do, Korea.

(*Received on September 25, 2001; accepted in final form on October 28, 2002*)

Hot compression test of up to 70 % reduction was performed to examine the effect of undercooling (ΔT=Ae_3−Ar_3) of austenite on strain induced ferrite (SIF) transformation behavior. The undercooling of austenite was controlled by applying various cooling rates from the austenitization temperature to the deformation temperature. In order to examine ferrite formation, the flow curve was measured and compared with the calculated flow stress of austenite. Fine ferrite grains with a size of 2 μm were observed within prior austenite grains. Increasing ΔT was an effective way to increase the amount of SIF, when the applied reduction was relatively small. With heavy deformation, the amount of SIF was nearly the same regardless of ΔT, while ferrite grains became finer and equiaxed by dynamic continuous recrystallization after transformation. It was also found that the amount of reduction for onset of ferrite formation within austenite grain was reduced with increasing ΔT. The decrease of flow stress was observed compared with that of austenite, which was mostly from ferrite formation during the deformation.

KEY WORDS: hot compression test; strain induced ferrite transformation; undercooling of austenite.

1. Introduction

Thermomechanical processing is very effective to refine ferrite grains to improve mechanical properties of low carbon steel.[1)] Recently, in order to obtain ultrafine ferrite grains, strain induced ferrite (SIF) by heavy deformation has been studied.[2–16)] However, SIF has not yet been applied to the plant scale rolling process, since more than 50 % reduction per single pass was required. Hodgson *et al.*[3,6)] noted that the high level of undercooling as well as the large amount of reduction was required to occur the strain induced ferrite transformation. However, the effect of undercooling on SIF transformation has not been studied in detail. The grain refinement of ferrite by heavy deformation was explained by the combination of dynamic transformation of ferrite and dynamic recrystallization of ferrite.[3–9)] Ferrite formation during the deformation was confirmed recently. Yada *et al.*[17)] reported that ferrite was formed during the deformation even above Ae_3 with para-equilibrium, which was analyzed by *in-situ* X-ray diffraction method. Grain refinement during the hot deformation could be attained either by discontinuous recrystallization or by continuous recrystallization.[18–23)] Hot deformation of metallic materials with low stacking fault energy such as austenite leads to the formation of new grain structure, that is, the occurrence of dynamic discontinuous recrystallization (DRX). On the other hand, it is generally considered that dynamic recovery is the main restoration of ferrite phase with high stacking fault energy rather than DRX.[20,21)] The dynamic continuous recrystallization is the phenomenon in which misorientation across sub-boundaries of ferrite increases continuously with increasing amount of strain until the sub-boundaries changes to high angle boundaries so that ferrite grains are subdivided. This process is further enhanced by dynamic recovery. However, the mechanism of SIF or ferrite grain refinement is still controversial.

In the present study, the effect of undercooling of austenite (ΔT) on SIF transformation was investigated. The high degree of undercooling was obtained with lowering the deformation temperature by applying high cooling rate. The evolution of SIF grains with deformation was examined by TEM. The formation of SIF was observed by stress-strain curve as well as microstructural examination.

2. Experimental Procedures

2.1. Specimen Preparation

A low carbon steel was prepared by VIM (Vacuum Induction Melting). The chemical composition of the steel used was shown in **Table 1**. Gleeble 1500 was used for hot compression test. Cylindrical samples with the diameter of 10 mm and length of 12 mm were machined from as-hot forged bars. A graphite foil with nickel compound was used

Table 1. Chemical compositions of the steel used.

(wt%)

C	Mn	Si	P	S
0.14	1.50	0.79	0.006	0.004

as a lubricant between WC (Tungsten carbide) anvil and specimen at high temperature. WC anvil was used to increase electric resistance at the interface of specimen so that uniform temperature along specimen axis was quickly obtained.

2.2. Hot Compression Test

Specimen was held at 1 100°C for 2 min and then cooled to the deformation temperature at a rate of 0.5, 2, 5 and 10°C s^{-1}. Hot compression test was carried out at Ar_3+10°C. The Ar_3 temperature was determined by measuring the first deviation of curvature of dilatation curve during continuous cooling. Specimen was compressed to 20, 30, 50, and 70% reduction at a strain rate of 10 s^{-1} respectively and then water quenched immediately. The microstructure of the quenched specimen was observed by optical microscope (OM) and transmission electron microscope (TEM). The volume fraction of the SIF and the average grain size were measured by an image analyzer. The misorientation angle between adjacent grains of ferrite was measured by Electron Back Scattered Diffraction (EBSD). Point to point analysis for adjacent grains was carried out. Area mapping for 28.4 μm×28.4 μm was performed with step size of 0.1 μm on square grid so that total step number was 80 656. The Inca crystal system was used with SEM (JSM-5900LV with tungsten filament-20 kV).

2.3. Measurement of Stress–Strain Curve

The flow stress of austenite at 1 100°C, 1 000°C and 900°C (T_d>Ae_3), of undercooled austenite at 800°C, 735°C (Ar_3<T_d<Ae_3) and of fully transformed structure at 735°C was measured. The fully transformed structure was obtained by isothermal holding at 735°C ($\alpha+\gamma$ region) for 10 min. The flow curve of austenite at 735°C was calculated by linear regression using the following equation[24] assuming the initial stage of measured flow stress solely originated from austenite.

$$\sigma = A\varepsilon^n \exp(B/\varepsilon) \quad \text{.....(1)}$$

The measured peak stress at various temperatures was compared with the peak stress calculated using the following equation.[25]

$$\sigma_p = (1/\alpha') \ln\{Y + (Y^2+1)^{1/2}\} \quad \text{.....(2)}$$

where, $Y=(Z/A)^{1/m}$ ($Z=\dot{\varepsilon}\exp(Q/RT)$).

Using the values formulated by Hatta *et al.*,[26] A, m, α' and Q were calculated as 1.09×10^{12} [s^{-1}], 5.47, 7.15×10^{-3} [MPa^{-1}] and 288.3 [kJ/mol] for 0.14 wt% C, respectively.

3. Results and Discussion

3.1. Degree of Undercooling (ΔT)

The degree of undercooling (ΔT) of austenite was defined as the difference between Ae_3 and Ar_3 temperature. The prior austenite grain size was 130 μm. The Ae_3 temperature was calculated as 844°C by Thermo-Calc. The Ar_3 temperatures with various cooling rates determined by dilatometry were shown in **Fig. 1** and **Table 2**. The Ar_3 was 751°C at a cooling rate of 0.5°C s^{-1} (ΔT=93°C) while it was 673°C at a cooling rate of 10°C s^{-1} (ΔT=171°C).

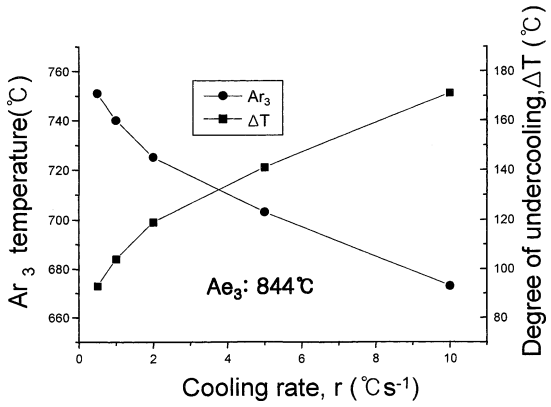

Fig. 1. Variation of Ar_3 and ΔT at various cooling rates.

Table 2. Measured Ar_3 temperatures and degree of undercooling (ΔT) with various cooling rates (Ae_3: 844°C).

Cooling rate	0.5℃/s	2℃/s	5℃/s	10℃/s
Ar_3	751℃	725℃	703℃	673℃
ΔT	93℃	119℃	141℃	171℃

3.2. Formation of Strain Induced Ferrite with Undercooling of Austenite (ΔT)

From the quenched specimen after 20% reduction, ferrite grains of about 5 μm were observed along g grain boundaries. After 30% reduction, fine ferrite grains with about 2 μm were observed within g grains as well as grain boundaries at larger ΔT, while they were not observed at the smaller ΔT as shown in **Fig. 2**. After 50% reduction, fine ferrite grains were observed within γ grains even at low ΔT. After 70% reduction, the amount of SIF apparently increased and its volume fraction reached about 65% regardless ΔT and the ferrite grain size was further refined as shown in **Fig. 3**. This indicated that the ferrite formation was more enhanced by the increase of nucleation site by heavy deformation.[27] The measured ferrite volume fraction and the calculated equilibrium volume fraction by Thermo-Calc with ΔT were shown in **Fig. 4**. The measured volume fraction of ferrite after 70% reduction was close to the equilibrium fraction of ferrite. The critical reduction for SIF was determined as onset of formation of fine ferrite grain with about 2 μm within g grain. **Figure 5** shows the critical reduction with ΔT. In the case where ΔT was 93°C (0.5°C s^{-1}), the critical reduction was 50%, while it was reduced to 30% when ΔT increased to 171°C (10°C s^{-1}). It was considered that the SIF was initiated by low reduction increasing ΔT.

3.3. Evolution of Strain Induced Ferrite during Hot Deformation

Figure 6 represents the evolution of strain induced ferrite grains during the hot deformation at 735°C (ΔT= 119°C). Although the amount of deformation increased, the ferrite grains formed at the early stage of deformation were equiaxed and their size was further refined as shown in Figs. 6(a) and 6(b). This phenomenon could be explained by dynamic continuous recrystallization of ferrite after transformation. Wang and Lei[18] reported that the misorientation across sub-boundaries of ferrite increased continu-

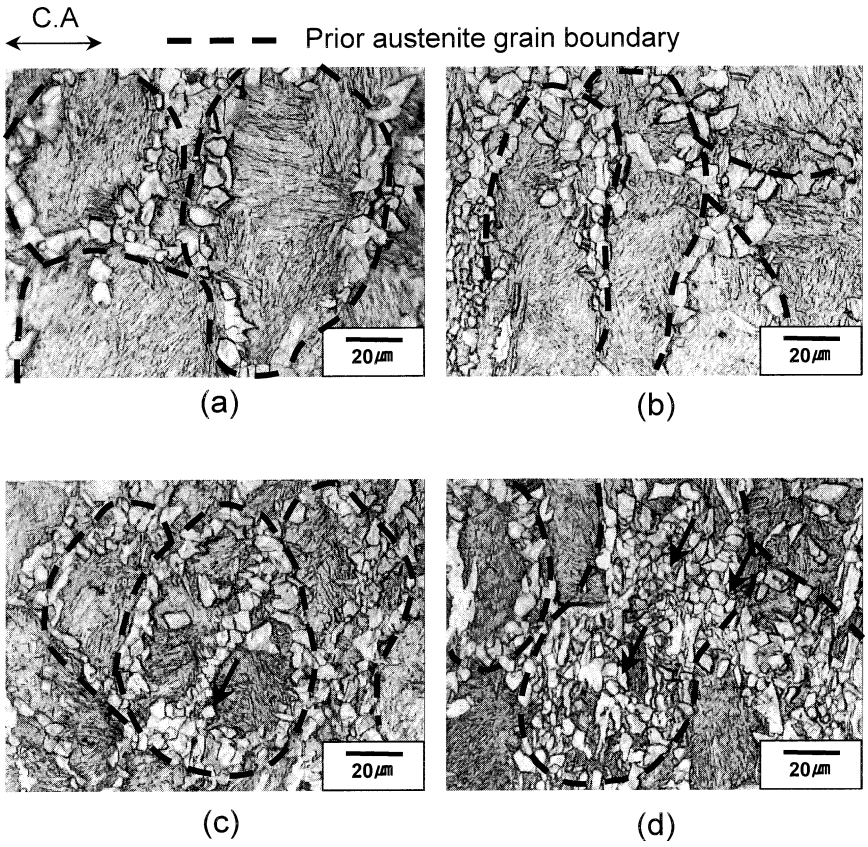

Fig. 2. Quenched microstructures after 30% reduction at $Ar_3+10°C$ for various ΔT.
(a) ΔT: 93°C (0.5°C s^{-1}), (b) ΔT: 119°C (2°C s^{-1}), (c) ΔT: 141°C (5°C s^{-1}), (d) ΔT: 171°C (10°C s^{-1}).

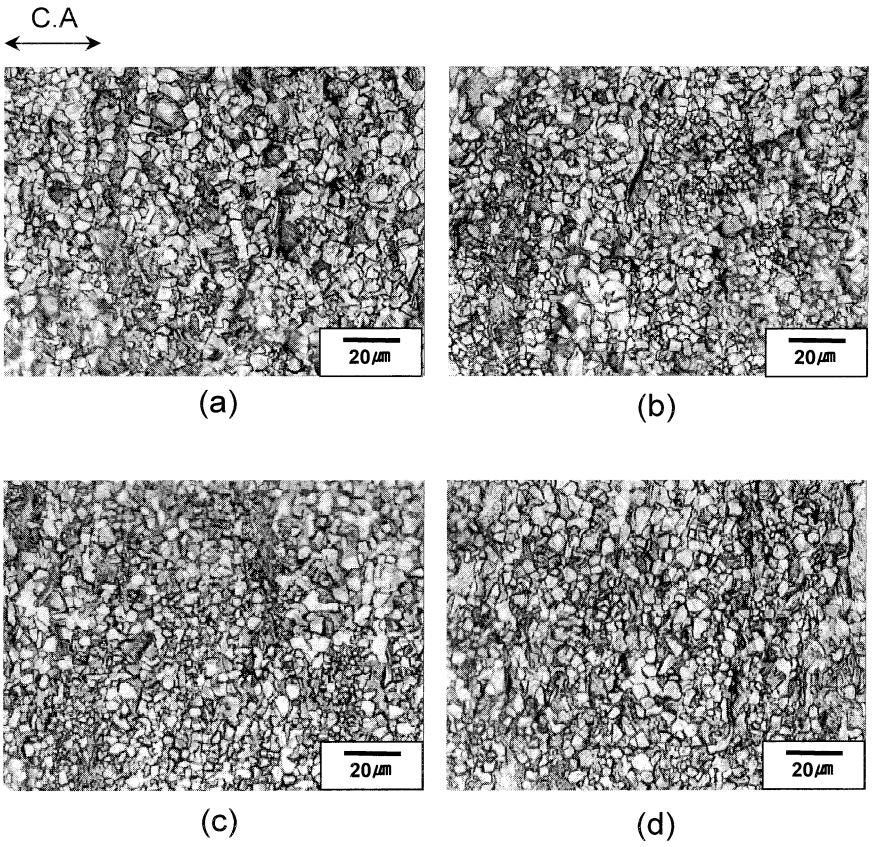

Fig. 3. Quenched microstructures after 70% reduction at $Ar_3+10°C$ for various ΔT.
(a) ΔT: 93°C (0.5°C s^{-1}), (b) ΔT: 119°C (2°C s^{-1}), (c) ΔT: 141°C (5°C s^{-1}), (d) ΔT: 171°C (10°C s^{-1}).

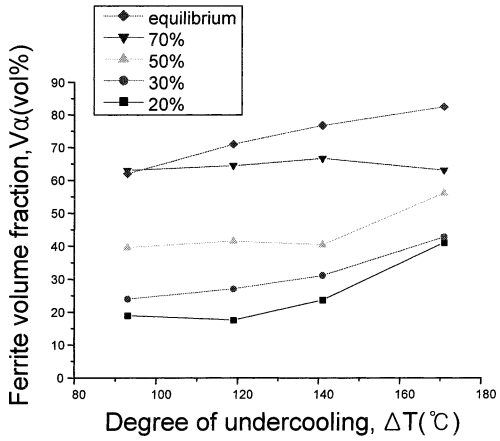

Fig. 4. Ferrite volume fraction as a function of degree of undercooling for various amounts of reduction.

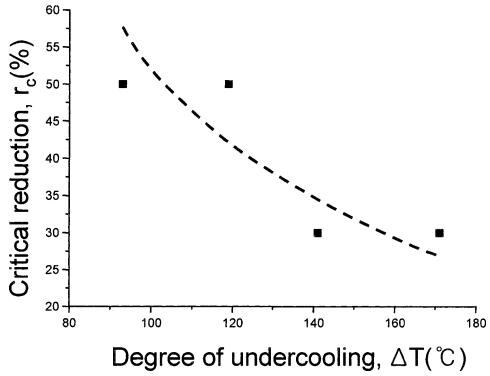

Fig. 5. Critical amount of reduction for onset of ferrite formation within austenite grain as a function of degree of undercooling.

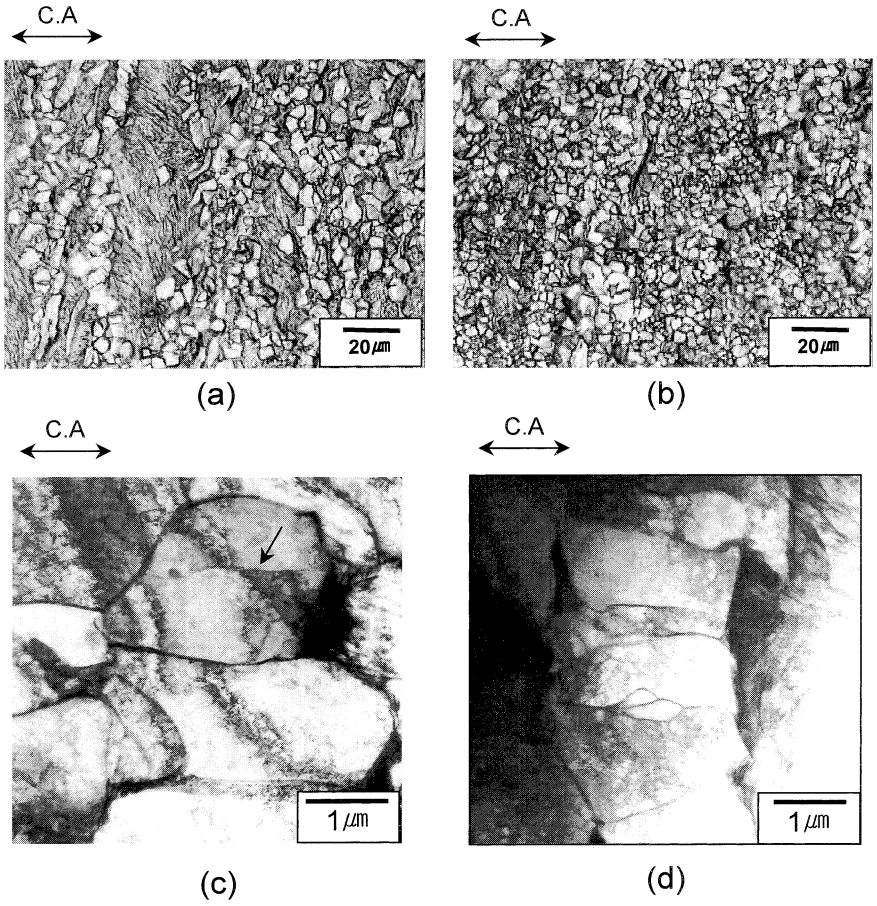

Fig. 6. Microstructures of strain induced ferrite with deformation at 735°C.
(a) 50% reduction (OM), (b) 70% reduction (OM), (c) 50% reduction (TEM), (d) 70% reduction (TEM).

ously with strain until the sub-boundaries were changed into high angle boundaries during the hot deformation (85% reduction) at strain rate of $10\,s^{-1}$ and at 800°C ($Z=4.3\times10^{14}\,s^{-1}$) in two phase ($\alpha+\gamma$) structure of low carbon steel. This is the so-called dynamic continuous recrystallization often observed in aluminum alloys or ferritic stainless steel,[19] and it is obviously different from the dynamic discontinuous recrystallization (DRX) found in high purity ferrite and in ferritic interstitial free steel where new grains were nucleated *via* the bulging of ferrite grain boundaries. According to previous studies,[22,23] DRX of ferrite occurred in interstitial free steel when the value of Z ($\dot{\varepsilon}\exp(Q/RT)$) was below $5\times10^{12}\,s^{-1}$ ($Q=280\,kJ\,mol^{-1}$). In the present study, the value of Z was $3.2\times10^{15}\,s^{-1}$ ($Q=280\,kJ\,mol^{-1}$) that was higher than that of possible Z for DRX even though the activation energy (Q) of low carbon steel was different from that of interstitial free steel. Thus, it was considered that further grain refinement was not caused by DRX of ferrite. The dynamic continuous recrystallization was mainly caused by absorption of dislocation into the sub-boundary of ferrite constrained by α/γ boundaries in two phase structure.[18] The phase boundary between strain induced ferrite and austenite played an important role to enhance the dynamic continuous recrystallization. Thus,

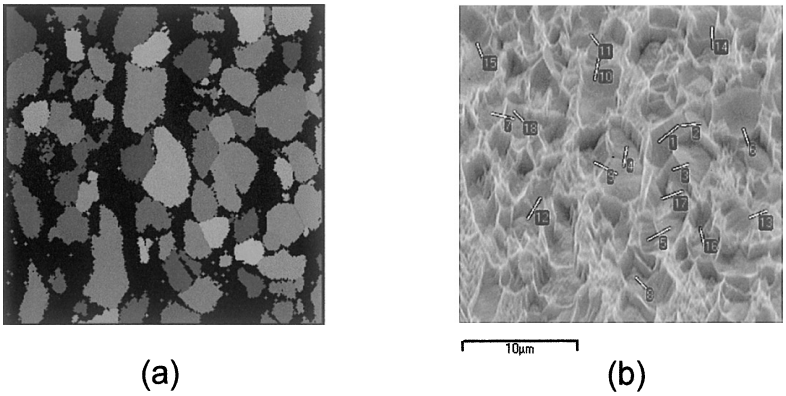

Line	Angle(°)
1	37.15
2	49.59
3	44.96
4	0.47
5	39.51
6	38.47
7	47.3
8	39.19
9	49.09
10	31.78
11	43.2
12	48.23
13	55.37
14	15
15	42.72
16	60.73
17	56.87
18	2.81

Fig. 7. Misorientation angle of strain induced ferrite grains formed by 70% reduction at 735°C. (a) Orientation map, (b) SEM image, (c) measured misorientation angle.

further grain refinement *via* dynamic continuous recrystallization took place by relatively low strain of 70% reduction. By TEM observation, the sub-grain boundaries were observed within equiaxed ferrite grains after 50% reduction as shown in Fig. 6(c). With increasing deformation to 70% reduction, further refined ferrite grains were observed along the prior austenite grain boundary or the deformation band within austenite grain as presented in Fig. 6(d). It was considered that sub-boundaries with low misorientation angle could be evolved to high angle boundaries resulting in subdivision of ferrite grains. As a result, ferrite grains formed at the early stage of deformation were not elongated by further deformation of 70% reduction. From point to point analysis by EBSD, these grain boundaries were composed of high angle boundaries and small amount of low angle boundaries as shown in **Fig. 7**. The similar result associated with misorientation angle of strain induced ferrite grains was reported.[6)]

3.4. Stress–Strain Curve

Figure 8 shows the calculated peak stress and measured peak stress of austenite with various deformation temperatures. At temperatures between 1 100°C and 900°C, the measured peak stress agreed well with the calculated one. When the deformation temperature was below 900°C, the measured peak stress was lower than calculated one for austenite. It indicated that the flow stress was reduced either by the formation of SIF or dynamic restoration. **Figure 9** shows the microstructures of quenched specimen at various temperatures after the deformation. The microstructures of the specimen quenched from 1 000°C and 900°C were fully martensite. While, SIF was observed at 800°C, which agreed with the analysis of peak stress. At 735°C, the large amount of SIF grains with about 2 μm were found within the austenite grain. From the microstructural examination, it was considered that the decrease of peak stress was mainly attributed by the formation of SIF rather than by dynamic restoration. Further, the flow stress at 735°C was calculated by linear regression of Eq. (2). It was assumed that the flow stress at the early stage of strain up to 0.3 was inherent to that of austenite.

$$\sigma_\gamma = 353.6\varepsilon^{0.19}\exp(-0.0247/\varepsilon), \quad R^2 = 0.99 \quad \text{.....(3)}$$

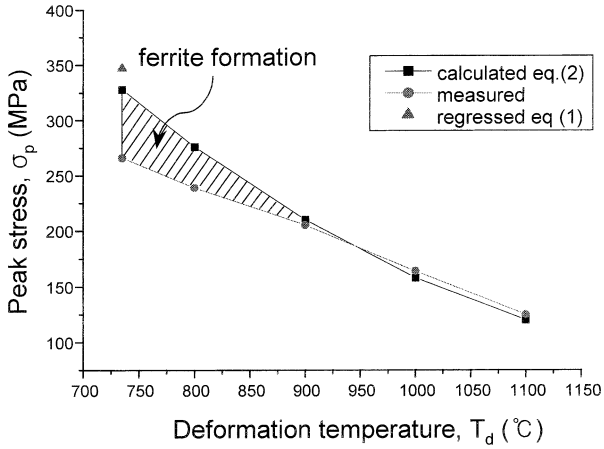

Fig. 8. Calculated peak stress for 70% reduction ($\dot{\varepsilon}=10\,s^{-1}$) with various deformation temperatures at a constant cooling rate of 2°C s^{-1}.

The measured stress–strain curve was lower than the calculated one (Eq. (3)) for austenite due to formation of SIF as shown in **Fig. 10**. In the case of deformation at 735°C after holding for 10 min, the stress–strain curve was much lower, since it was partly attributed to flow stress of coarse ferrite grains with size of 40 μm formed during the isothermal holding as well as flow stress of austenite.[28)] From the above results, it was thought that ferrite formation during the deformation reduced the flow stress.

4. Conclusions

(1) The SIF with ultrafine grain size of 2 μm was obtained by the combination of ΔT and amount of deformation. It was also found that the amount of reduction for onset of ferrite formation within austenite grain was reduced with increasing ΔT. With 70% reduction, the ferrite volume fraction was close to the equilibrium volume fraction regardless of ΔT.

(2) The SIF grains were finer and were maintained to be equiaxed even though the deformation increased. It was considered that ferrite grains transformed at the early stage of deformation were subdivided by dynamic continuous recrystallization.

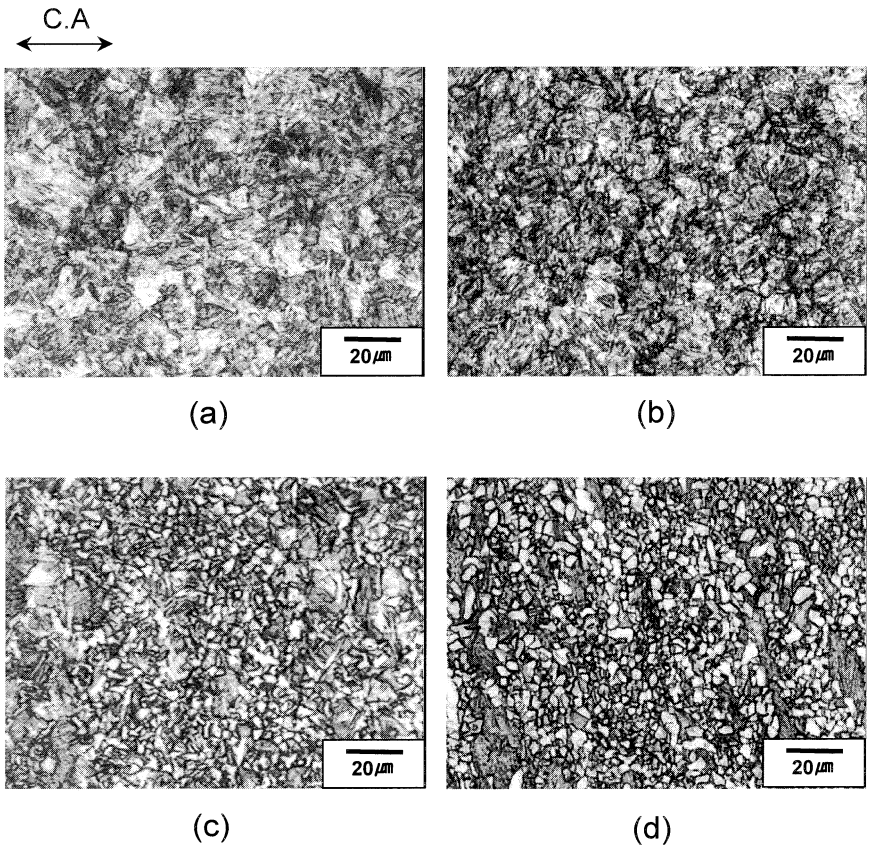

Fig. 9. Quenched microstructures after 70% reduction ($\dot{\varepsilon}=10\,s^{-1}$) at various temperatures during continuous cooling at $2°C\,s^{-1}$.
(a) 1 000°C, (b) 900°C, (c) 800°C, (d) 735°C.

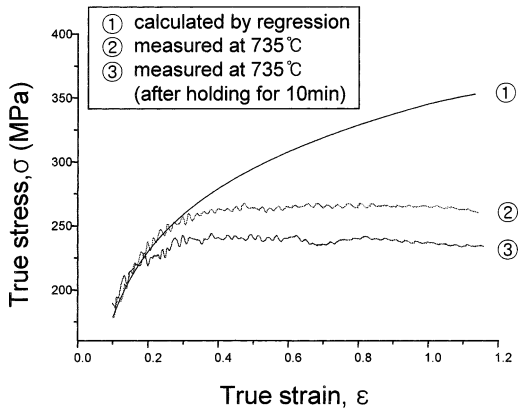

Fig. 10. Measured flow curves compared with calculated flow curve using Eq. (1) for 735°C.

(3) The measured flow stress between Ae_3 and Ar_3 temperature was lower than the calculated one for austenite. This indicated that ferrite was formed during the deformation and this was also confirmed by microstructural examination.

REFERENCE

1) F. B. Pickering: Physical Metallurgy and Design of Steels, Applied Science Publishers Ltd., Barking, Essex, United Kingdom, (1978), 64.
2) W. Y. Choo: *J. Korean Inst. Met. Mater.*, **36** (1998), No. 11, 1966.
3) P. D. Hodgson, M. R. Hickson and R. K. Gibbs: *Scr. Metall. Mater.*, **40** (1999), No. 10, 1179.
4) M. Niikura, M. Fujioka, Y. Adachi, A. Matsukura, T. Yokota, Y. Shirota and Y. Hagiwara: *J. Mater. Process. Technol.*, **117** (2001), 341.
5) P. J. Hurley and P. D. Hodgson: *Mater. Sci. Eng. A*, **302** (2001), 206.
6) S. Lee, D. Kwon, Y. K. Lee and O. Kwon: *Metall. Trans. A*, **26A** (1995), 1093.
7) K. Nagai: J. *Mater. Process. Technol.*, **117** (2001), 329.
8) Z. Q. Sun, W. Y. Yang, J. J. Qi and A. M. Hu: *Mater. Sci. Eng.*, **A334** (2002), 201.
9) Y. D. Huang and L. Froyen: *J. Mater. Process. Technol.*, **124** (2002), 216.
10) E. Essadiqi and J. J. Jonas: *Metall. Trans. A*, **19A** (1988), 417.
11) B. Mintz, J. Lewis and J. J. Jonas: *Mater. Sci. Technol.*, **13** (1997), 379.
12) Y. Matsumura and H. Yada: *Tetsu-to-Hagané*, **69** (1983), 1460.
13) C. Ouchi and K. Matsumoto: *Trans. Iron Steel Inst. Jpn.*, **22** (1982), 181.
14) H. Yada, N. Matsuzu and K. Nakajima: *Trans. Iron Steel Inst. Jpn.*, **23** (1983), 100.
15) H. G. Suzuki, S. Nishimura and J. Imamura: *Trans. Iron Steel Inst. Jpn.*, **24** (1984), 169.
16) S. T. Hong: Proc. of the 2nd Workshop on The Development of High Performance Structural Steels for 21th Century, Vol. 2, POSCO, Pohang, (1999), C-1.
17) H. Yada, C.-M. Li and H. Yamagata: *ISIJ Int.*, **40** (2000), 200.
18) R. Z. Wang and T. C. Lei: *Scr. Mater.*, **31** (1994), No. 9, 1193.
19) A. Belyahov, R. Kaibyshev and T. Sakai: *Metall. Trans. A*, **29A** (1998), 161.
20) H. J. McQueen: *Metall. Trans. A*, **8A** (1977), 807.
21) E. Inoue and T. Sakai: *J. Jpn. Inst. Met.*, **55** (1991), 286.
22) G. Glover and C. M. Sellars: *Metall. Trans. A*, **4A** (1973), 765.
23) N. Tsuji, Y. Matsubara and Y. Saito: *Scr. Mater.*, **37**, (1997), No. 4, 477.
24) T. Spittel and M. Spittel: *Scand. J. Metall.*, **19** (1990), 85.
25) T. Sakai and M. Ohashi: *Tetsu-to-Hagané*, **67**, (1981), No 11, 2000.
26) N. Hatta, J. Kokado, S. Kikuchi and H. Takuda: *Steel Res.*, **56** (1985), 575.
27) M. Umemoto and I. Tamura: Proc. of Int. Conf. on HSLA Steels, TMS, Warrendale, PA, (1985), 373.
28) J. Perttula and P. Karjalainen: S*teel Res.*, **68** (1997), No. 3, 115.